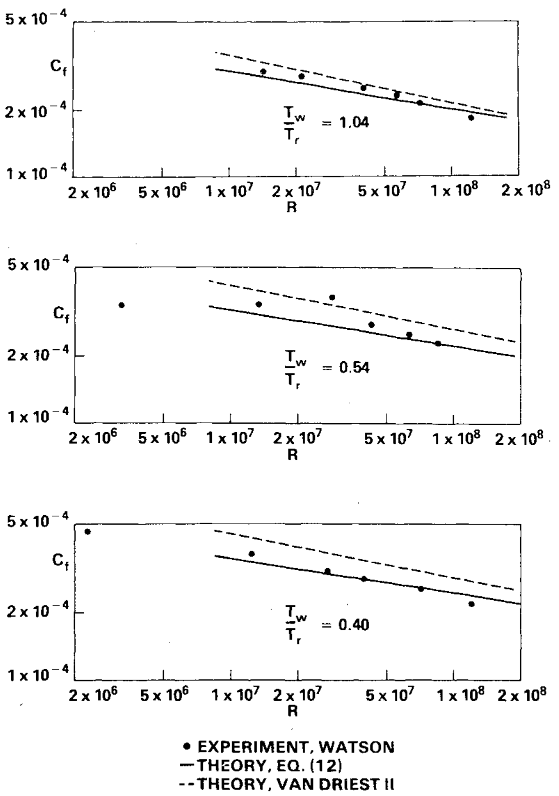

Fig. 3 Comparison of theory and experiment: helium, $M_I = 11.3$, $r = 0.883$.

lowest wall temperature ratio, $T_w/T_r = 0.40$, the agreement between Eq. (12) and experiment is excellent. In this case the data fall well below the Van Driest II result. At the higher wall temperatures, the data fall between Eq. (12) and Van Driest II. However, at the higher Reynolds numbers, where any error in the virtual origin has the least effect, Eq. (12) agrees best with the data.

References

[1]Wilson, R. E., "Turbulent Boundary-Layer Characteristics at Supersonic Speeds—Theory and Experiment," *Journal of the Aeronautical Sciences*, Vol. 17, Sept. 1950, pp. 585-594.

[2]Van Driest, E. R., "Turbulent Boundary Layer in Compressible Fluids," *Journal of the Aeronautical Sciences*, Vol. 18, March 1951, pp. 145-216.

[3]Van Driest, E. R., "The Problem of Aerodynamic Heating," *Aero. Aspects Session, National Summer Meeting, IAS*, Los Angeles, Calif., June 1956.

[4]Hopkins, E. J., Keener, E. R., and Dwyer, H. A., "Turbulent Skin Friction and Boundary-Layer Profiles Measured on Nonadiabatic Flat Plates at Hypersonic Mach Numbers," AIAA Paper 71-167, Jan. 1971; also *AIAA Journal*, Vol. 10, Jan. 1972, pp. 40-48.

[5]Coles, D., "The Turbulent Boundary Layer in a Compressible Fluid," *The Physics of Fluids*, Vol. 7, Sept. 1964.

[6]Sommer, S. C. and Short, B. J., "Free-Flight Measurements of Turbulent-Boundary-Layer Skin Friction in the Presence of Severe Aerodynamic Heating at Mach Numbers from 2.8 to 7.0," NACA TN 3391, 1955.

[7]Spalding, D. B. and Chi, S. W., "The Drag of a Compressible Turbulent Boundary Layer on a Smooth Flat Plate with and without Heat Transfer," *Fluid Mechanics*, Vol. 18, Jan. 1964, pp. 117-143.

[8]Watson, R. D., "Wall Cooling Effects on Hypersonic Transitional/Turbulent Boundary Layers at High Reynolds Numbers," *AIAA Journal*, Vol. 15, Oct. 1977, pp. 1455-1461.

[9]von Kármán, Th., "Mechanische Ahnlichkeit and Turbulenz," *Proceedings of the 3rd International Congress for Applied Mechanics*, Vol. I, Aug. 29, 1930, pp. 85-92; see also von Kármán, Th., "Mechanical Similitude and Turbulence, NACA TM No. 611, March 1931.

[10]Wilson, R. E., "Turbulent Boundary-Layer Temperature Profiles and Reynolds Analogy," *International Journal of Heat and Mass Transfer*, Vol. 21, Aug. 1978, pp. 1167-1170.

[11]Harkness, J. L., "The Effect of Heat Transfer on Turbulent Boundary Layer Skin Friction," Defense Research Laboratory, University of Texas, DRL Rept. 436, CM-940, June 1959.

[12]Schoenherr, K. E., "Resistance of Flat Surfaces Moving Through a Fluid," *Transactions of the Society of Naval Architectures and Marine Engineering*, Vol. 40, 1932, pp. 279-313.

Effect of Frequency in Unsteady Transonic Flow

Donald P. Rizzetta* and Wilson C. Chin*
The Boeing Company, Seattle, Wash.

Introduction

A CHARACTERISTIC of transonic unsteady flows is the potentially large phase lag between boundary motion and induced surface pressure. Moreover, net force coefficients generally exceed those in subsonic and supersonic speed regimes. These effects tend to increase the likelihood of aeroelastic instabilities, making transonic speeds most critical for aircraft flutter. In this Note the effects of frequency are systematically considered within the framework of transonic small-disturbance theory for three different configurations: airfoil pitching oscillation, trailing edge flap oscillation, and impulsive change to angle of attack. An approximate factorization method applicable to general unsteady motions is devised to study the net lift and moment coefficients for the NACA 64A010 airfoil section, at Mach 0.82 and for three reduced frequencies, namely, 0.05, 0.5, and 5.0. The results are then compared against those obtained in the low-frequency approximation.

Generally speaking, small surface motions can induce large changes in aerodynamic loading, as well as large increments in shock excursion. These considerations arise from the inherent nonlinearity of the mathematical problem. Thus, in the numerical sense, direct time integration, which does not bear the limiting restriction to "frozen" shock movements, typical of linearized approaches, must be used. In the low-frequency approximation, solutions to the transonic small-disturbance equation, along these lines, simulate well the expected flow nonlinearity, including irregular shockwave motions.[1-3] These results compare well with those obtained from the unsteady Euler equations and are in good agreement with experiment. However, the restriction to low frequencies may, in practice, be severe; more rapid oscillations, as well as unsteady gust loadings, are excluded from consideration. The essential loss is that in phase-shift information and it is remedied by retaining in the governing equations the high-frequency terms. This forms the substance of the numerical algorithm discussed in this Note. Of course, the extent to which the low-frequency approximation holds is also of fundamental interest, and comparisons are given for this purpose. This is obviously important in assessing the effect of frequency on transonic phase shifts and bears practical significance on direct aeroelastic applications.

Received March 20, 1979.

Index categories: Nonsteady Aerodynamics; Transonic Flow; Computational Methods.

*Specialist Engineer, Aerodynamics Research Group. Member AIAA.

Numerical Procedure

We consider the nondimensional equation:

$$A\phi_{\tau\tau}+2B\phi_{\xi\tau}=C\phi_{\xi\xi}+\phi_{\eta\eta} \tag{1}$$

where ϕ is a disturbance velocity potential normalized by $cU_\infty\delta^{2/3}$, c being the chord, U_∞ the freestream speed at infinity, and δ the maximum thickness-to-chord ratio. Let ω be an oscillation frequency and define a reduced frequency by $k=\omega c/U_\infty$. If M_∞ is the freestream Mach number, the coefficients appearing in Eq. (1) are $A=k^2M_\infty^2/\delta^{2/3}$, $B=kM_\infty^2/\delta^{2/3}$ and $C=(1-M_\infty^2)/\delta^{2/3}-(\gamma+1)M_\infty^2\phi_\xi$, where γ is the ratio of specific heats, nondimensional coordinates having been assumed in the form $\tau=U_\infty kt/c$, $\xi=x/c$, and $\eta=\delta^{1/3}y/c$, x,y, and t being streamwise, transverse, and time variables. For small k, A vanishes, and Eq. (1) leads to the low-frequency approximation. In general, Eq. (1) is solved together with $\phi_\eta(\xi,0^\pm,\tau)=f_\xi^\pm+akf_\tau^\pm$ along the chord $0\le\xi\le1$, where $f^\pm$ is an instantaneous airfoil displacement normalized by δ, with $a=0$ in the low-frequency limit and $a=1$ in the general case. In addition, pressure continuity is enforced across the wake aft of the trailing edge, and disturbance velocities are assumed to vanish at infinity. The unsteady pressure coefficient is evaluated from $C_p=-2\delta^{2/3}(\phi_\xi+ak\phi_\tau)$.

Solutions to Eq. (1) were obtained by a noniterative alternating-direction-implicit (ADI) scheme used to advance the solution for ϕ at each meshpoint from time level t_n to time level t_{n+1} through the following sequential procedure:

$$\xi\text{-sweep:}\quad \frac{2B}{\Delta\tau}\delta_\xi(\tilde{\phi}-\phi^n)=D_\xi g+\delta_{\eta\eta}\phi^n \tag{2a}$$

$$\eta\text{-sweep:}\quad \frac{A}{(\Delta\tau)^2}\{\phi^{n+1}-2\phi^n+\phi^{n-1}\}$$

$$+\frac{2B}{\Delta\tau}\delta_\xi(\phi^{n+1}-\tilde{\phi})=\tfrac{1}{2}\delta_{\eta\eta}(\phi^{n+1}-\phi^n) \tag{2b}$$

where $g=\tfrac{1}{2}(C^n\tilde{\phi}_\xi+(1-M_\infty^2)\phi_\xi^n/\delta^{2/3})$. This decomposition is a consistent approximate factorization of Eq. (1) accurate to $0(\Delta\tau)$. In the low-frequency limit, it reduces to the LTRAN2 algorithm described in Ref. 1, the latter method being second-order accurate in time and unconditionally stable on a von Neumann basis.[2] For general unsteady motions, the present scheme, GTRAN2, while not unconditionally stable, appears to be quite reliable, and instabilities were not observed in the current run portfolio. Note that $\delta_{\eta\eta}$ denotes the central difference operator, δ_ξ the backward difference streamwise operator, and D_ξ the mixed difference operator discussed in Ref. 1. Details related to the implementation of tangency, wake, and farfield conditions, as well as those for correct shock capture, for brevity, will not be referenced here, these being straightforward modifications to LTRAN2.

Results

Comparisons of low- and general-frequency solutions to Eq. (1) for the NACA 64A010 airfoil section were made at Mach 0.82 for three types of unsteady motions: airfoil pitching oscillation, trailing edge flap oscillation, and impulsive change in angle of attack. All time integrations were initiated at $\tau=0$ with a ϕ distribution corresponding to the steady-state solution. In these comparisons, all solutions were obtained using identical spatial mesh distributions and spatial differencing; in addition, the time step sizes in GTRAN2 and LTRAN2 were chosen so that $\Delta\tau_G\cong\Delta\tau_L^2$, making the truncation errors formally of the same order. Generated solutions used 360 time steps for GTRAN2 and 48 time steps for LTRAN2 per period of oscillation at any reduced frequency.

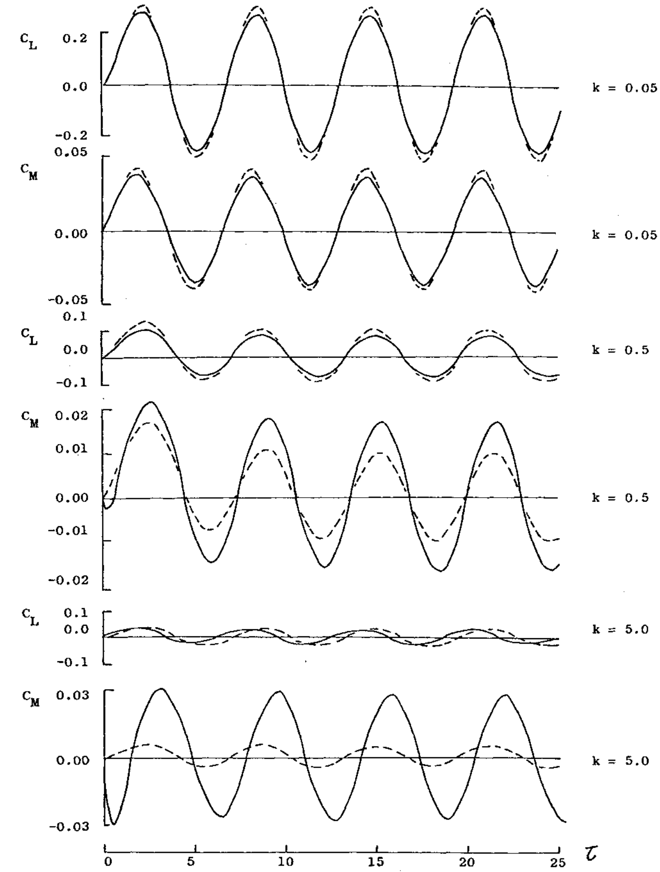

Fig. 1 Pitch oscillations (see Fig. 2 for α history), GTRAN2——, LTRAN2------.

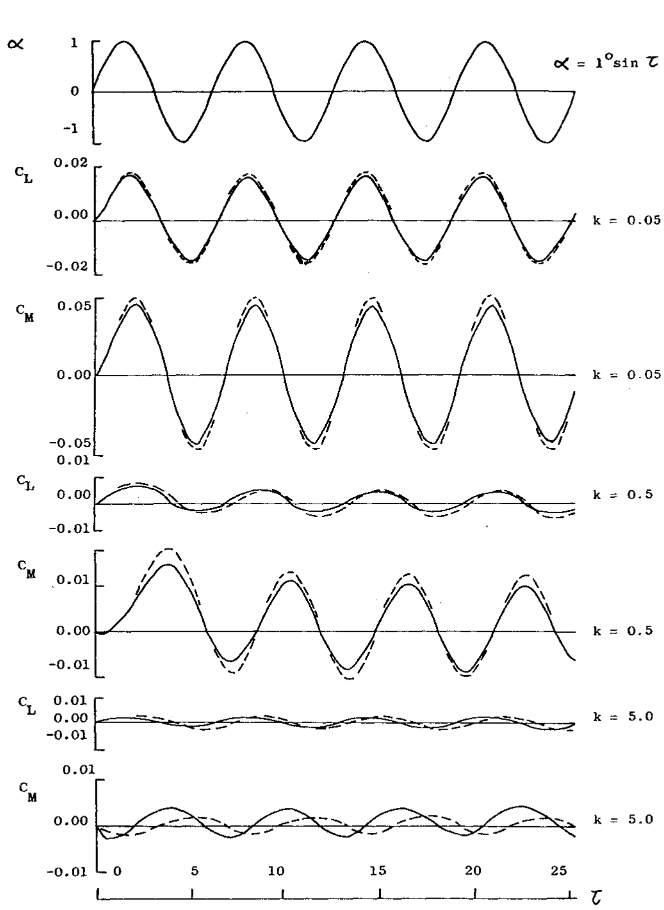

Fig. 2 Flap oscillations, GTRAN2——, LTRAN2----.

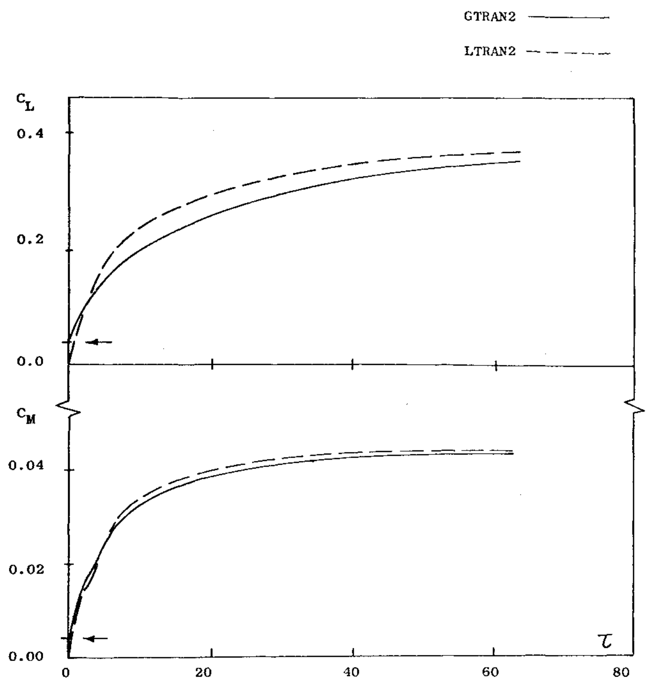

Fig. 3 Impulsive change in angle of attack.

Results obtained using both larger and smaller $\Delta\tau$ increments indicated that these choices adequately insured numerical accuracy. A nonuniform computational mesh consisting of 113 ξ and 97 η points, with 48 points lying over the chord was used. Minimum grid spacings were $\Delta\xi = 0.0025$ and $\Delta\eta = 0.01$ with the computation box defined by $200.0 > |\xi|$ and $397.8 > |\eta|$.

Oscillation cases were time integrated over four periods for $k = 0.05$, 0.5, and 5.0. Figure 1 compares low- and general-frequency results for a $\alpha = \pm 1$ deg airfoil pitching oscillation about the midchord for the unsteady lift and pitching moment coefficients (the moment is taken about the pitch point). At $k = 0.05$, the results are similar except that peak C_L's and C_M's are slightly overpredicted by the low-frequency approximation. With $k = 0.5$, the results appear to agree in phase, but amplitudes differ by about 30%. At $k = 5.0$, a phase difference of about 45 deg is observed in addition to differences in predicted amplitude levels. As k increases, there is a reduction in lift due to a decrease in the shock excursion; the moment, however, remains high because of the shock traversing the pitch point. Physical considerations suggest that shock excursion amplitudes decrease with increasing k. This is confirmed numerically in both models; decay rates in LTRAN2, however, far exceed those observed in GTRAN2. Figure 2 compares results for a $\alpha = \pm 1$ deg trailing edge flap oscillation about $\xi = 0.75$. Results for $k = 0.05$ are similar to those for airfoil oscillation. For $k = 0.5$, however, the low-frequency result overpredicts the moment, unlike the airfoil oscillation case. The lift and moment are substantially lower for the flap oscillation than for the airfoil oscillation case due to the presence of a shock lying upstream of the unsteady disturbance. Finally, we considered impulsive changes in angle of attack from 0-1 deg. The time response to such a step change is often used in modeling gusts or for performing aeroelastic calculations by the indicial method.[3] Time histories for the lift and moment taken about midchord appear in Fig. 3 where $k = 1.0$. For small time, the general-frequency solution shows an abrupt increase in both C_L and C_M. This agrees qualitatively with solutions of the Euler equations[4]; however, this is not obtained in the low-frequency approximation. Apparently the high-frequency components of the unsteady disturbance are critical during this transient period. Both solutions however tend to the same asymptote.

Concluding Remarks

An ADI scheme for general unsteady motions is developed requiring only simple modifications to LTRAN2. Computed results for three different problems indicate the importance of the unsteady terms in high-frequency and gustlike motions. For the cases considered, good agreement was found for low reduced frequencies. For these problems, LTRAN2 is more cost efficient.

Acknowledgment

The authors are grateful to W. F. Ballhaus and P. M. Goorjian for making LTRAN2 available for their use and to H. Yoshihara for some helpful discussions.

References

[1] Ballhaus, W. F. and Goorjian, P. M., "Implicit Finite-Difference Computations of Unsteady Transonic Flows About Airfoils," *AIAA Journal*, Vol. 15, Dec. 1977, pp. 1728-1735.

[2] Ballhaus, W. F. and Steger, J. L., "Implicit Approximate Factorization Schemes for the Low-Frequency Transonic Equation," NASA TMX-73,082, Nov. 1975.

[3] Ballhaus, W. F. and Goorjian, P. M., "Calculation of Unsteady Transonic Flows by the Indicial Method," *AIAA Journal*, Vol. 16, Feb. 1978, pp. 117-124.

[4] Magnus, R. J., "Calculation of Some Unsteady Transonic Flows About the NACA 64A006 and 64A010 Airfoils," AFFDL-TR-77-46, July 1977.

Transport Physics and Mathematical Characteristics

Gustave Hokenson*
Biphase Energy Systems, Santa Monica, Calif.

FLUID dynamic computations of continuum flows are usually based on the hypothesis that the molecular dynamics are in equilibrium with the local macroscopic flowfield state.[1,2] Within this framework, determination of the analytical form of the stress tensor and transport coefficients (for sufficiently dilute media) traditionally relies on Chapman-Enskog solutions to the Boltzmann equation.[3] These relate the transport coefficients to local thermodynamic variables and provide linear algebraic relationships between transport fluxes and the spatial gradients of relevant macroscopic flowfield variables.[4] Higher order transport effects[5-7] that modify linear algebraic theory have not received much attention in continuum flows, inasmuch as the required flowfield time constant becomes significantly smaller than that which is generally established. However, various solutions of Boltzmann's equation in rarefied gases[6] inherently include nonequilibrium effects that are confirmed experimentally.

Results of computations carried out utilizing gradient transport modeling have been verified for a wide range of conditions and are generally accepted. There are, however, mathematical consequences peculiar to the use of these diffusive models. Of primary importance are the infinite "signal" propagation speed and the associated asymptotic nature of solutions to the resultant conservation relations.

Received Nov. 2, 1978; revision received Feb. 20, 1979.

Index categories: Supersonic and Hypersonic Flow, Boundary Layers and Convective Heat Transfer—Laminar, Rarefied Flows.

*Manager of Research, Subsidiary of Research-Cottrell. Member AIAA.